

II. QUANTUM INTERFERENCE OF ENTANGLED PHOTONS

We consider the interferometric scheme implemented by Kalashnikov *et al.*¹⁶ A CW laser beam is incident on a nonlinear crystal, creating an entangled photon pair state by spontaneous parametric down-conversion (SPDC), which we shall denote as a Bell state

$$|\blacklozenge_1\rangle = \iint d\omega_1 d\omega_2 \mathcal{F}(\omega_1, \omega_2) B_S^\dagger(\omega_1) B_I^\dagger(\omega_2) |0\rangle, \quad (1)$$

where $\mathcal{F}(\omega_1, \omega_2)$ is the bi-photon field amplitude and $B_{S,I}^\dagger(\omega_i)$ creates a photon with frequency ω_i in either the signal or idler branch. The ket $|0\rangle$ is the vacuum state and $|\omega_1 \omega_2\rangle$ denotes a two photon state.

In general, energy conservation requires that the entangled photons generated by spontaneous parametric down conversion (SPDC) obey $\omega_L = \omega_1 + \omega_2$. Similarly, conservation of photon momentum requires $\mathbf{k}_L = \mathbf{k}_1 + \mathbf{k}_2$. By manipulating the SPDC crystal, one can generate entangled photon pairs with different frequencies. As a result, the bi-photon field is strongly anti-correlated in frequency with

$$|\blacklozenge\rangle = \int dz \mathcal{F}(z) B_1^\dagger(\omega_L - z) B_2^\dagger(\omega_L + z) |0\rangle, \quad (2)$$

where ω_L is the central frequency of the bi-photon field. This aspect was recently exploited in Ref.¹⁵, which used a visible photon in the idler branch and an infrared (IR) photon in the signal branch, interacting with the sample.

As sketched in Figure 1, both signal and idler are reflected back towards a beam-splitter (BS) by mirrors M1 and M2 and the signal mode further interacts with a sample at S.

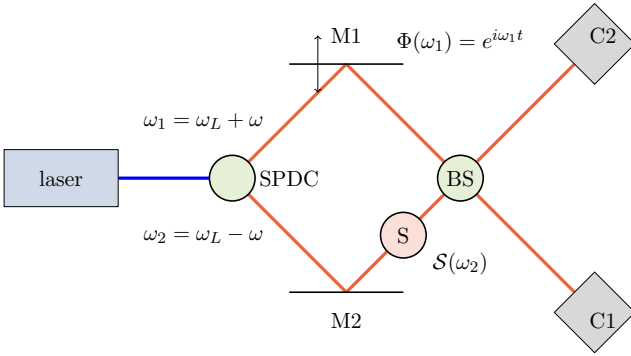


FIG. 1. **Sketch of Hong-Ou-Mandel apparatus (HOM) for 2-photon coincidence detection.** The initial laser beam pass through a spontaneous parametric down-conversion crystal (SPDC) creating an entangled photon pair which is split into idler (ω_1) and signal (ω_2) modes. The two beams are subsequently reflected back towards a beam-splitter (BS) by mirrors M1 and M2 and the signal mode further interacts with a sample at S. The modes are recombined by a beam-splitter (BS) and directed towards coincidence counters C1 and C2. Not shown in our sketch is an optional pumping laser for creating a steady-state exciton density in S.

and M2. M1 introduces an optical delay with transmission function $\Phi(\omega)$ which we will take to be of modulo 1. In the other arm, we introduce a resonant medium at S with transmission function $\mathcal{S}(\omega)$. Not shown in our sketch is an optional pumping laser for creating a steady state exciton density in S.

Upon interacting with both the delay element and the medium, the Bell-state can be rewritten as

$$|\blacklozenge_2\rangle = \iint d\omega_1 d\omega_2 \mathcal{F}(\omega_1, \omega_2) B_I^\dagger(\omega_1) B_S^\dagger(\omega_2) \Phi(\omega_1) \mathcal{S}(\omega_2) |0\rangle. \quad (3)$$

Finally, the two beams are recombined by a beam splitter (BS) and the coincidence rate is given by

$$\begin{aligned} P_c &= \iint d\omega_1 d\omega_2 |\langle \omega_1 \omega_2 | \psi_c \rangle|^2 \\ &= \frac{1}{4} \iint d\omega_1 d\omega_2 \{ |\mathcal{F}(\omega_1, \omega_2) \mathcal{S}(\omega_2)|^2 + |\mathcal{F}(\omega_2, \omega_1) \mathcal{S}(\omega_1)|^2 \\ &\quad - 2\text{Re} [\mathcal{F}^*(\omega_1, \omega_2) \mathcal{F}(\omega_2, \omega_1) \mathcal{S}^*(\omega_2) \mathcal{S}(\omega_1) \Phi^*(\omega_1) \Phi(\omega_2)] \} \end{aligned}$$

We assume that the delay stage is dispersionless with $\Phi(\omega) = e^{i\omega t}$ and re-write equation 4 as

$$\begin{aligned} P_c(t_{\text{delay}}) &= \frac{1}{4} \int_{-\infty}^{+\infty} dz |\mathcal{F}(z)|^2 \{ |\mathcal{S}(\omega_L - z)|^2 + |\mathcal{S}(\omega_L + z)|^2 \\ &\quad - 2\text{Re} [\mathcal{S}^*(\omega_L - z) \mathcal{S}(\omega_L + z) e^{-2izt_{\text{delay}}}] \}, \quad (5) \end{aligned}$$

where t_{delay} is the time lag between entangled photons traversing the upper and lower arms of the HOM apparatus. This is proportional to the counting rate of coincident photons observed at detectors C1 and C2 and serves as the central experimental observable.

III. RESULTS

A crucial component of our approach is the action of the sample at S which introduces a transmission function $\mathcal{S}(\omega)$ into the final Bell state. We wish to connect this function to the dynamics and molecular interactions within the sample. To accomplish this, we use the input/output formulation of quantum optics and apply this to an ensemble of identical 2-level states coupled to a common photon mode.²⁴ Technical details of our approach are presented in the Methods section of this paper. In short, we begin with a description of the material system described by N two-level spin states coupled to common set of photon cavity modes.

$$\begin{aligned} \hat{H}_{sys} &= \sum_j \frac{\hbar\omega_o}{2} \hat{\sigma}_{z,j} + \sum_k \hbar(\omega_k - i\kappa) \hat{\psi}_k^\dagger \hat{\psi}_k \\ &\quad + \sum_{k,j} \frac{\hbar\lambda_{kj}}{\sqrt{N}} (\hat{\psi}_k^\dagger + \hat{\psi}_k) (\hat{\sigma}_j^+ + \hat{\sigma}_j^-) \end{aligned} \quad (6)$$

where $\{\hat{\sigma}_{z,j}, \hat{\sigma}_j^\pm\}$ are local spin-1/2 operators for site j , $\hbar\omega_o$ is the local excitation energy, and λ_{kj} is the coupling between the k th photon mode and the j th site, which we

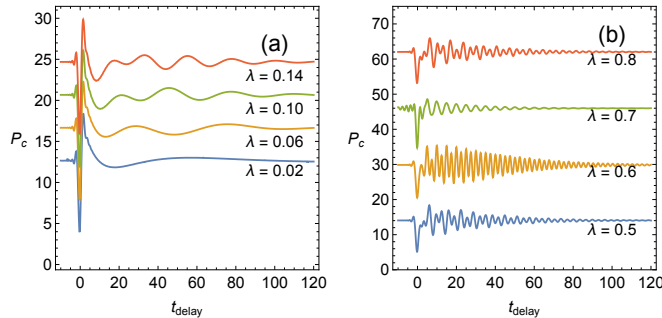


FIG. 2. **Photon Coincidence Rates vs. Coupling.** We compare here the computed (relative) coincidence counting rates as λ increases from weak (a) to strong coupling (b). As throughout this work we take $\lambda_c = 0.7516$ as per equation 9. Each scan is shifted vertically for clarity.

will take to be uniform over all sites. We introduce κ as the decay rate of a cavity photon. We allow the photons in the cavity (S) to exchange quanta with photons in the HOM apparatus and derive the Heisenberg equations of motion corresponding to input and output photon fields within a steady state assumption. This allows us to compute the scattering matrix connecting an incoming photon with frequency ν from the field to an outgoing photon with frequency ν returned to the field viz.

$$\Psi_{out}(\nu) = -\hat{\Omega}_{out}^{(-)\dagger} \hat{\Omega}_{in}^{(+)} \Psi_{in}(\nu) \quad (7)$$

where $\hat{\Omega}_{in,out}^{(\pm)}$ are Møller operators that propagate an incoming (or outgoing) state from $t \rightarrow -\infty$ to $t = 0$ where it interacts with the sample. or from $t = 0$ to an outgoing (or incoming) state at $t \rightarrow +\infty$ and give the S -matrix in the form of a response function

$$\mathcal{S}(\nu) = \langle \delta\Psi_{out}^\dagger(\nu) \delta\Psi_{out}(\nu') \rangle \delta(\nu - \nu') \quad (8)$$

where the $\delta\Psi_{out}(\nu)$ are fluctuations in the output photon field about a steady-state solution. The derivation of $\mathcal{S}(\nu)$ for the Dicke model and its incorporation into equation 5 is a central result of this work and is presented in the Methods section of this paper. In general, $\mathcal{S}(\nu)$ is a complex function with a series of poles displaced above the real ν axis and we employ a sync-transformation method to integrate equation 5. The approach can be applied to any model Hamiltonian system and provides the necessary connection between a microscopic model and its predicted photon coincidence.

Before discussing the results of our calculations, it is important to recapitulate a number of aspects of the Dicke model and how these features are manifest in the photon coincidence counting rates. As stated already, we assume that the sample is in a steady state by exchanging the photons in the HOM apparatus with photons within the sample cavity and that $\mathcal{S}(\nu)$ can be described within a linear-response theory. Because the cavity photons become entangled with the material excitations, the excitation frequencies are split into upper photonic (ω_+) and lower excitonic (ω_-) branches. These frequencies

are complex corresponding to the exchange rate between cavity and HOM photons.

At very low values of λ_k , the real frequencies are equal and $\omega_+ = \omega_-$. In this over-damped regime, photons leak from the cavity before the photon/exciton state has undergone a single Rabi oscillation. At $\lambda_k = \kappa/2$ the system becomes critically damped and for $\lambda_k < \kappa/2$ and the degeneracy between the upper and lower polariton branches is lifted. As λ_k increases above a critical value given by

$$\lambda_c = \sqrt{\frac{\omega_k \omega_o}{4} \left(1 + \frac{\kappa^2}{\omega_k^2} \right)}, \quad (9)$$

the system undergoes a quantum phase transition when $\omega_- = 0$. Above this regime, excitations from the non-equilibrium steady-state become collective and super-radiant. For our numerical results, unless otherwise noted we use dimensionless quantities, taking $\omega_o = \omega_k = 1.5$ for both the exciton frequency and cavity mode frequency, $\kappa = 0.05$ for the cavity decay. These give a critical value of $\lambda_c = 0.7516$.

We first consider the photon coincidence in the normal regime. Figures 2(a,b) show the variation of the photon coincidence count when the laser frequency is resonant with the excitons ($\omega_k = \omega_o$). For low values of λ_k , the system is in the over-damped regime and the resulting coincidence scan reveals a slow decay for positive values of the time-delay. This is the perturbative regime in which the scattering photon is dephased by the interaction with the sample, but there is insufficient time for the photon to become entangled with the sample. For $\lambda_k > \kappa/2$, the scattering photon is increasingly entangled with the material and further oscillatory structure begins to emerge in the coincidence scan.

In the strong coupling regime, $P_c(t)$ becomes increasingly oscillatory with contributions from multiple frequency components. The origin of the structure is further revealed upon taking the Fourier cosine transform of $P_c(t)$ (equation 5) taking the bandwidth of the bi-photon amplitude to be broad enough to span the full spectral range. The first two terms in the integral of equation 5

are independent of time and simply give a background count and can be ignored for purpose of analysis. The third term depends upon the time delay and is Fourier-cosine transform of the bi-photon amplitude times the scattering amplitudes,

$$\mathcal{P}_c(\omega) = |\mathcal{F}(\omega)|^2 \mathcal{S}^*(\omega_L - \omega) \mathcal{S}(\omega_L + \omega). \quad (10)$$

As we show in the Methods, $\mathcal{S}(\omega)$ has a series of poles on the complex plane that correspond to the frequency spectrum of fluctuations about the matter-radiation steady-state as given by the eigenvalues of \mathcal{M}_s in equation C8 in the Methods. In Figure 3(a,b) we show the evolution of pole-structure of $\mathcal{S}^*(\omega_L - z) \mathcal{S}(\omega_L + z)$ superimposed over the Fourier-cosine transform of the coincidence counts ($\mathcal{P}_c(\omega)$) with increasing coupling λ_k revealing that both excitonic and photonic branches contribute to the overall photon coincidence counting rates.

A close examination of the pole structure in the vicinity of the phase transition reveals that two of the $\omega_k^{(-)}$ modes become degenerate over a small range of λ_k but with different imaginary components indicating that the two modes decay at different rates. This is manifest in Figure 3b by the rapid variation and divergence in the $\mathcal{S}^*(\omega_L - z) \mathcal{S}(\omega_L + z)$ about λ_c .²⁵ While the parametric width of this regime is small, it depends entirely upon the rate of photon exchange between the cavity and the laser field (κ).

IV. DISCUSSION

We present here a formalism and method for connecting the photon coincidence signals for a sample placed in a HOM apparatus to the optical response of the coupled photon/material system. Our formalism reveals that by taking the Fourier transform of the $P_c(t)$ coincidence signal reveals the underlying pole structure of the entangled material/photon system. Our idea hinges upon an assumption that the interaction with the material preserves the initial entanglement between the two photons and that sample on the entanglement introduces an additional phase lag to one of the photons which we formally introduce in the form of a scattering response function \mathcal{S} . The pole-structure in the output comes about from the further quantum entanglement of the signal photon with the sample.

Encoded in the time-delay signals is important information concerning the inner-workings of a quantum phase transition. Hence, we conclude that entangled photons with interferometric detection techniques provide a viable and tractable means to extract precise information concerning light-matter interactions. In particular, the approach reveals that at the onset of the symmetry-breaking transition between normal and super-radiant phases, two of the eigenmodes of the light-matter state

exhibit distinctly different lifetimes. This signature of an intrinsic aspect of light-matter entanglement may be observed in a relatively simple experimental geometry with what amounts to a *linear* light-scattering/interferometry set up.

At first glance, it would appear that using quantum photons would not offer a clear advantage over more standard spectroscopies based upon a semi-classical description of the radiation field. However, the entanglement variable adds an additional dimension to the experiment allowing one to preform what would ordinarily be a non-linear experiment using classical light as a linear experiment using quantized light. The recent works by Kalashnikov *et al.* that inspired this work are perhaps the proverbial tip of the iceberg.^{15,16}

ACKNOWLEDGMENTS

The work at the University of Houston was funded in part by the National Science Foundation (CHE-1664971, MRI-1531814) and the Robert A. Welch Foundation (E-1337). AP acknowledges the support provided by Los Alamos National Laboratory Directed Research and Development (LDRD) Funds. CS acknowledges support from the School of Chemistry & Biochemistry and the College of Science of Georgia Tech. JJ acknowledges the support of the Army Research Office (W911NF-13-1-0162). ARSK acknowledges funding from EU Horizon 2020 via Marie Skłodowska Curie Fellowship (Global) (Project No. 705874).

Appendix A: Preparation of Entangled States

We review here the preparation of the entangled states as propagated to the coincidence detectors in Fig. 1. The initial laser beam produces an entangled photon pair by spontaneous parametric down-conversion at B, with state which we shall denote as a Bell state

$$|\bullet_1\rangle = \iint d\omega_1 d\omega_2 \mathcal{F}(\omega_1, \omega_2) B_I^\dagger(\omega_1) B_S^\dagger(\omega_2) |0\rangle \quad (A1)$$

$$= \iint d\omega_1 d\omega_2 \mathcal{F}(\omega_1, \omega_2) |\omega_1 \omega_2\rangle, \quad (A2)$$

where $\mathcal{F}(\omega_1, \omega_2)$ is the bi-photon field amplitude and $B_{I,S}^\dagger(\omega_i)$ creates a photon with frequency ω_i in either the idler (I) or signal (S) arm of the HOM apparatus. The ket $|0\rangle$ is the vacuum state and $|\omega_1 \omega_2\rangle$ denotes a two photon state. The two photons are reflected back towards a beam-splitter (BS) by mirrors M1 and M2. M1 introduces an optical delay with transmission function $\Phi(\omega)$ which we will take to be of modulo 1. In the other arm, we introduce a resonant medium at S with transmission function $\mathcal{S}(\omega)$.

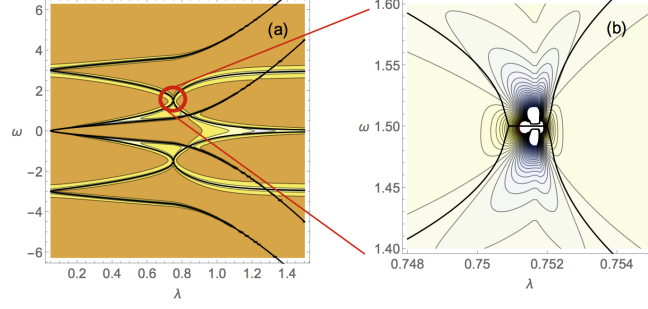


FIG. 3. **Pole Structure of Response Function.** (a) Contour plot of $\mathcal{P}_c(\omega)$ (Eq.10) varying the coupling λ . Superimposed are the locations of the (real) poles of the spectral response $\mathcal{S}^*(\omega_L - \omega)\mathcal{S}(\omega_L + \omega)$. (b) Expansion of the intersection between ω_- branches in the critical regime showing the rapid variation of the response in this region.

Upon interacting with both the delay element and the medium, the Bell-state can be rewritten as

$$|\blacktriangle_2\rangle = \iint d\omega_1 d\omega_2 \mathcal{F}(\omega_1, \omega_2) B_I^\dagger(\omega_1) B_S^\dagger(\omega_2) \Phi(\omega_1) S(\omega_2) |0\rangle. \quad (\text{A3})$$

Finally, the two beams are re-joined by a beam-splitter (BS) producing the mapping

$$B_I^\dagger(\omega_1) B_S^\dagger(\omega_2) \mapsto \frac{1}{2} [A_1^\dagger(\omega_1) + iA_2^\dagger(\omega_1)] [A_2^\dagger(\omega_2) + iA_1^\dagger(\omega_2)]$$

whereby $A_i^\dagger(\omega_j)$ creates a photon with frequency ω_j in the i^{th} exit channel. This yields a final Bell state

$$\begin{aligned} |\blacktriangle_{out}\rangle = & \frac{1}{2} \iint d\omega_1 d\omega_2 \mathcal{F}(\omega_1, \omega_2) \left((A_1^\dagger(\omega_1) A_2^\dagger(\omega_2) - A_2^\dagger(\omega_1) A_1^\dagger(\omega_2)) \right. \\ & \left. + i (A_1^\dagger(\omega_2) A_1^\dagger(\omega_1) + A_2^\dagger(\omega_1) A_2^\dagger(\omega_2)) \right) \Phi(\omega_1) S(\omega_2) |0\rangle. \end{aligned} \quad (\text{A4})$$

The coincidence count rate is determined only by the real part of photon creation term, so we write

$$\begin{aligned} |\blacktriangle_c\rangle = & \frac{1}{2} \int d\omega_1 \int d\omega_2 (\mathcal{F}(\omega_1, \omega_2) \Phi(\omega_1) S(\omega_2) \\ & - \mathcal{F}(\omega_2, \omega_1) \Phi(\omega_2) S(\omega_1)) |\omega_1 \omega_2\rangle \end{aligned} \quad (\text{A5})$$

and

$$\begin{aligned} P_c = & \iint d\omega_1 d\omega_2 |\langle \omega_1 \omega_2 | \psi_c \rangle|^2 \\ = & \frac{1}{4} \iint d\omega_1 d\omega_2 \{ |\mathcal{F}(\omega_1, \omega_2) \mathcal{S}(\omega_2)|^2 + |\mathcal{F}(\omega_2, \omega_1) \mathcal{S}(\omega_1)|^2 \\ & - 2\text{Re}[\mathcal{F}^*(\omega_1, \omega_2) \mathcal{F}(\omega_2, \omega_1) \mathcal{S}^*(\omega_2) \mathcal{S}(\omega_1) \Phi^*(\omega_1) \Phi(\omega_2)] \}. \end{aligned} \quad (\text{A6})$$

Upon taking $\omega_1 = \omega_L + \omega$ and $\omega_2 = \omega_L - \omega$, and changing the integration variable we obtain equation 5 in the text.

Appendix B: Input/Output formalism

Our theoretical approach is to treat S as a material system interacting with a bath of quantum photons. We shall denote our “system” as those degrees of freedom describing the material and the photons directly interacting with the sample, described by H_{sys} and assume that the photons within sample cavity are exchanged with external photons in the bi-photon field,

$$H_r + H_{rs} = \hbar \int_{-\infty}^{\infty} \left\{ z B_k^\dagger(z) B_k(z) - i\kappa(z) (\psi_k^\dagger B_k(z) - B_k^\dagger(z) \psi_k) \right\} dz, \quad (\text{B1})$$

where $[B_k(z), B_{k'}^\dagger(z')] = \delta_{kk'} \delta(z - z')$ are boson operators for photons in the laser field, and $[\psi_k, \psi_{k'}^\dagger] = \delta_{kk'}$ are boson operators for cavity photons in the sample that directly interact with the material component of the system.

The Heisenberg equations of motion for the reservoir and system photon modes are given by

$$\partial_t B_k(z) = -izB_k(z) + \kappa(z)\psi_k \quad (\text{B2})$$

and

$$\partial_t \psi_k = -\frac{i}{\hbar}[\psi_k, H_{sys}] - \int \kappa(z)B_k(z;t)dz, \quad (\text{B3})$$

where the integration range is over all z . We can integrate formally the equations for the reservoir given either the initial or final states of the reservoir field

$$B_k(z;t) = \begin{cases} e^{-iz(t-t_i)}B_k(z;t_i) + \kappa(z)\int_{t_i}^t ds e^{-iz(t-s)}\psi_k(s) & \text{for } t > t_i \\ e^{-iz(t-t_f)}B_k(z;t_f) - \kappa(z)\int_t^{t_f} ds e^{-iz(t-s)}\psi_k(s) & \text{for } t < t_f. \end{cases} \quad (\text{B4})$$

We shall eventually take $t_i \rightarrow -\infty$ and $t_f \rightarrow +\infty$ and require that the forward-time propagated and reverse-time propagated solutions are the same at some intermediate time t . If we assume that the coupling is constant over the frequency range of interest, we can write

$$\kappa(z) = \sqrt{\gamma/2\pi}$$

where γ is the rate that energy is exchanged between the reservoir and the system. This is the (first) Markov approximation.

Using these identities, one can find the Heisenberg equations for the cavity modes as

$$\partial_t \psi_k = -\frac{i}{\hbar}[\psi_k, H_{sys}] - \sqrt{\frac{\gamma}{2\pi}} \int_{-\infty}^{+\infty} B_k(z;t)dz \quad (\text{B5})$$

where H_{sys} is the Hamiltonian for the isolated system. We can now cast the external field in this equation in terms of its initial condition:

$$\begin{aligned} \partial_t \psi_k &= -\frac{i}{\hbar}[\psi_k, H_{sys}] - \sqrt{\frac{\gamma}{2\pi}} \int_{-\infty}^{+\infty} e^{iz(t-t_i)} B_{k0}(z)dz \\ &\quad - \frac{\gamma}{2\pi} \int_{-\infty}^{+\infty} dz \int_{t_i}^t e^{iz(t-t')} \psi_k(t') dt' \end{aligned} \quad (\text{B6})$$

Let us define an input field in terms of the Fourier transform of the reservoir operators:

$$\psi_{k,in}(t) = -\frac{1}{\sqrt{2\pi}} \int_{-\infty}^{+\infty} dz e^{-iz(t-t_i)} B_{k0}(z). \quad (\text{B7})$$

Since these depend upon the initial state of the reservoir, they are essentially a source of stochastic noise for the system. In our case, we shall use these as a formal means to connect the fields inside the sample to the fields in the laser cavity.

For the term involving $\gamma/2\pi$, the integral over frequency gives a delta-function:

$$\int_{-\infty}^{\infty} dz e^{iz(t-t')} = 2\pi\delta(t-t'). \quad (\text{B8})$$

then

$$\int_{t_o}^t dt' \delta(t-t') \psi_k(t') = \frac{\psi_k(t)}{2} \text{ for } (t_o < t < t_f) \quad (\text{B9})$$

This gives the forward equation of motion.

$$\partial_t \psi_k = -\frac{i}{\hbar}[\psi_k, H_{sys}] + \sqrt{\gamma}\psi_{k,in}(t) - \frac{\gamma}{2}\psi_k(t) \quad (\text{B10})$$

We can also define an output field by integrating the reservoir backwards from time t_f to time t given a final state of the bath, B_{kf} .

$$B_k = e^{-iz(t-t_f)} B_{kf} - \sqrt{\frac{\gamma}{2\pi}} \int_t^{t_f} e^{-iz(t-t')} \psi_k(t') dt' \quad (\text{B11})$$

This produces a similar equation of motion for the output field

$$\partial_t \psi_k = -\frac{i}{\hbar}[\psi_k, H_{sys}] - \sqrt{\gamma}\psi_{k,out}(t) + \frac{\gamma}{2}\psi_k(t) \quad (\text{B12})$$

Upon integration:

$$\psi_{k,out}(t) = \frac{1}{\sqrt{2\pi}} \int_{-\infty}^{+\infty} d\nu e^{-i\nu(t-t_f)} B_{kf}(\nu). \quad (\text{B13})$$

At the time t , both equations must be the same, so we can subtract one from the other

$$\psi_{k,in} + \psi_{k,out} = \sqrt{2\kappa}\psi_k \quad (\text{B14})$$

to produce a relation between the incoming and outgoing components. This eliminates the non-linearity and explicit reference to the bath modes.

We now write $\Psi = \{\psi_k, \psi_k^\dagger, S_1, S_2, \dots\}$ as a vector of Heisenberg variables for the material system $\{S_1, S_2, \dots\}$ and cavity modes $\{\psi_k, \psi_k^\dagger\}$. Taking the equations of motion for the all fields to be linear and of the form

$$\partial_t \Psi = \mathcal{M}_{in} \cdot \Psi + \sqrt{\gamma}\Psi_{in} \quad (\text{B15})$$

where \mathcal{M}_{in} is a matrix of coefficients which are independent of time. The input vector Ψ_{in} is non-zero for only

the terms involving the input modes. We can also write a similar equation in terms of the output field; however, we have to account for the change in sign of the dissipation terms, so we denote the coefficient matrix as \mathcal{M}_{out} . In this linearized form, the forward and reverse equations of motion can be solved formally using the Laplace transform, giving

$$(\mathcal{M}_{in} - iz)\Psi(z) = -\sqrt{\gamma}\Psi_{in}(z) \quad (\text{B16})$$

$$(\mathcal{M}_{out} - iz)\Psi(z) = +\sqrt{\gamma}\Psi_{out}(z). \quad (\text{B17})$$

These and the relation $\Psi_{in} + \Psi_{out} = \sqrt{\gamma}\Psi$ allows one to eliminate the external variables entirely:

$$\Psi_{out}(z) = -(\mathcal{M}_{out} - iz)(\mathcal{M}_{in} - iz)^{-1}\Psi_{in}(z). \quad (\text{B18})$$

This gives a precise connection between the input and output fields. More over, the final expression does not depend upon the assumed exchange rate between the internal ψ_k and external $B_k(z)$ photon fields. The procedure is very much akin to the use of Møller operators in scattering theory. To explore this connection, define $\hat{\Omega}_{in}^{(\pm)}$ as an operator which propagates an incoming solution at $\mp\infty$ to the interaction at time $t = 0$ and its reverse $\hat{\Omega}_{out}^{(\pm)}$ which propagates an out-going solution at $\mp\infty$ back to the interaction at time $t = 0$.

$$\hat{\Omega}_{in,out}^{(\pm)\dagger}\hat{\Omega}_{in,out}^{(\pm)} = I, \quad (\text{B19})$$

and

$$\hat{\Omega}_{in}^{(\pm)} = (\mathcal{M}_{in} \mp iz)^{-1} \quad (\text{B20})$$

$$\hat{\Omega}_{out}^{(\pm)} = (\mathcal{M}_{out} \pm iz)^{-1} \quad (\text{B21})$$

Thus, we can write equation B18 as

$$\Psi_{out}(z) = -\hat{\Omega}_{out}^{(-)\dagger}\hat{\Omega}_{in}^{(+)}\Psi_{in}(z). \quad (\text{B22})$$

To compute the response function, we consider fluctuations and excitations from a steady state solution:

$$\Psi(t) = \Psi_{ss} + \delta\Psi(t). \quad (\text{B23})$$

The resulting linearized equations of motion read

$$\frac{d}{dt}\delta\Psi(t) = \mathcal{M}_s\delta\Psi(t) \quad (\text{B24})$$

implying a formal solution of

$$\delta\Psi(t) = e^{\mathcal{M}_s t}\delta\Psi(0). \quad (\text{B25})$$

From this we deduce that the eigenvalues and eigenvectors of \mathcal{M}_s give the fluctuations in terms of the normal excitations about the stationary solution. Using the input/output formalism, we can write the outgoing state (in terms of the Heisenberg variables) in terms of their input values:

$$\delta\Psi_{out}(z) = -(\mathcal{M}_{out,s} - izI)(\mathcal{M}_{in,s} - izI)^{-1}\delta\Psi_{in}(z) \quad (\text{B26})$$

where as given above, $\delta\Psi(z)$ is a vector containing the fluctuations about the stationary values for each of the

Heisenberg variables. The $\mathcal{M}_{in,s}$ and $\mathcal{M}_{out,s}$ are the efficient matrices from the linearisation process. The input field satisfies $\langle\delta\psi_{in}(z)\delta\psi_{in}^\dagger(z')\rangle = \delta(z - z')$ and all other terms are zero. Thus, the transmission function is given by

$$\delta(z - z')\mathcal{S}(z) = \langle\delta\psi_{out}^\dagger(z)\delta\psi_{out}(z')\rangle \quad (\text{B27})$$

In other words, the $\mathcal{S}(z)$ is the response of the system to the input field of the incoming photon state producing an output field for the out-going photon state.

Appendix C: Dicke model for ensemble of identical emitters

Let us consider an ensemble of N identical two-level systems corresponding to local molecular sites coupled to a set of photon modes described by ψ_k .

$$\begin{aligned} \hat{H} = & \sum_j \frac{\hbar\omega_o}{2}\hat{\sigma}_{z,j} + \sum_k \hbar\omega_k\hat{\psi}_k^\dagger\hat{\psi}_k \\ & + \sum_{k,j} \frac{\hbar\lambda_{kj}}{\sqrt{N}}(\hat{\psi}_k^\dagger + \hat{\psi}_k)(\hat{\sigma}_j^+ + \hat{\sigma}_j^-) \end{aligned} \quad (\text{C1})$$

where $\{\hat{\sigma}_{z,j}, \hat{\sigma}_j^\pm\}$ are local spin-1/2 operators for site j , $\hbar\omega_o$ is the local excitation energy, and λ_{kj} is the coupling between the k th photon mode and the j th site, which we will take to be uniform over all sites. Defining the total angular momentum operators

$$\hat{J}_z = \sum_j \hat{\sigma}_{z,j} \quad \text{and} \quad \hat{J}_\pm = \sum_j \hat{\sigma}_j^\pm$$

and

$$\hat{J}^2 = \hat{J}_z^2 + (\hat{J}_+\hat{J}_- + \hat{J}_-\hat{J}_+)/2$$

as the total angular momentum operator, this Hamiltonian can be cast in the form in equation C1 by mapping the total state space of N spin 1/2 states onto a single angular momentum state vector $|J, M\rangle$.

$$\begin{aligned} \hat{H} = & \hbar\omega_o\hat{J}_z + \sum_k \hbar\omega_k\hat{\psi}_k^\dagger\hat{\psi}_k \\ & + \sum_k \frac{\hbar\lambda_k}{\sqrt{N}}(\hat{\psi}_k^\dagger + \hat{\psi}_k)(\hat{J}_+ + \hat{J}_-) \end{aligned} \quad (\text{C2})$$

Note that the ground state of the system corresponds to $|J, -J\rangle$ in which each molecule is in its electronic ground state. Excitations from this state create up to N excitons within the system corresponding to the state $|J, +J\rangle$. Intermediate to this are multi-exciton states which correspond to various coherent superpositions of local exciton configurations. For each value of the wave vector k one obtains the following Heisenberg equations of motion for the operators

$$\frac{\partial\hat{\psi}_k}{\partial t} = (-i\omega_k - \kappa)\hat{\psi}_k - i\frac{\lambda_k}{\sqrt{N}}(\hat{J}_+ + \hat{J}_-) \quad (\text{C3})$$

$$\frac{\partial \hat{\psi}_k^\dagger}{\partial t} = (i\omega_k - \kappa)\hat{\psi}_k^\dagger + i\frac{\lambda_k}{\sqrt{N}}(\hat{J}_+ + \hat{J}_-) \quad (\text{C4})$$

$$\frac{\partial \hat{J}_\pm}{\partial t} = \pm i\omega_o \hat{J}_\pm \mp 2i\hat{J}_z \sum_k \frac{\lambda_k}{\sqrt{N}}(\hat{\psi}_k + \hat{\psi}_k^\dagger) \quad (\text{C5})$$

$$\frac{\partial \hat{J}_z}{\partial t} = +i\frac{\hbar\lambda_k}{\sqrt{N}}(\hat{J}_- - \hat{J}_+)(\hat{\psi}_k + \hat{\psi}_k^\dagger) \quad (\text{C6})$$

where κ is gives the decay of photon $\hat{\psi}_k$ into the reservoir. These are non-linear equations and we shall seek stationary solutions and linearize about them.

$$\frac{d}{dt}\delta\Psi(t) = \mathcal{M}_s\delta\Psi(t) \quad (\text{C7})$$

with

$$\mathcal{M}_s = \begin{bmatrix} -(\kappa - i\omega_k) & 0 & i\lambda_k & i\lambda_k & 0 \\ 0 & -(\kappa + i\omega_k) & -i\lambda_k & -i\lambda_k & 0 \\ 2i\lambda_k\bar{J}_z & 2i\lambda_k\bar{J}_z & -i\omega_o & 0 & 2i\lambda_k(\bar{\psi}_k + \bar{\psi}_k^\dagger) \\ -2i\lambda_k\bar{J}_z & -2i\lambda_k\bar{J}_z & 0 & i\omega_o & -2i\lambda_k(\bar{\psi}_k + \bar{\psi}_k^\dagger) \\ i\lambda_k(\bar{J}_- - \bar{J}_+) & i\lambda_k(\bar{J}_- - \bar{J}_+) & i\lambda_k(\bar{\psi}_k + \bar{\psi}_k) & -i\lambda_k(\bar{\psi}_k + \bar{\psi}_k) & 0 \end{bmatrix} \quad (\text{C8})$$

where $\bar{J}_{z,\pm}$, $\bar{\psi}_k$, and $\bar{\psi}_k^\dagger$ denote the steady state solutions. Where we have removed N from the equations of motion by simply rescaling the variables. The model has both trivial and non-trivial stationary solutions corresponding to the normal and super-radiant regimes. For the normal regime,

$$\bar{\psi}_k = \bar{\psi}_k^\dagger = \bar{J}_{\pm,s} = 0 \quad (\text{C9})$$

and

$$\bar{J}_z = \pm \frac{N}{2}. \quad (\text{C10})$$

which correspond to the case where every spin is excited or in the ground state. Since we are primarily interested in excitations from the electronic ground state, we initially focus our attention to these solutions.

Non-trivial solutions to these equations predict that above a critical value of the coupling $\lambda > \lambda_c$, the system will undergo a quantum phase transition to form a super-radiant state. It should be pointed out that in the original Dicke model, above the critical coupling, the system is no longer gauge invariant leading to a violation of the Thomas-Reiche-Kuhn (TRK) sum rule. Gauge invariance can be restored; however, the system no longer undergoes a quantum phase transition.²⁶ However, for a *driven, non-equilibrium* system such as presented here, the TRK sum rule does not apply and the quantum phase transition is a physical effect.

The non-trivial solutions for the critical regime are given by

$$\bar{\psi}_k^2 = (\bar{\psi}_k^\dagger)^2 = \frac{1}{4} \frac{\omega_k \lambda_k^2}{\omega_o \lambda_c^2} \left(1 - \left(\frac{\lambda_c}{\lambda_k} \right)^4 \right) \quad (\text{C11})$$

$$\bar{J}_\pm = \frac{1}{2} \left(1 - \left(\frac{\lambda_c}{\lambda_k} \right)^4 \right)^{1/2} \quad (\text{C12})$$

$$\bar{J}_z = -\frac{1}{2} \left(\frac{\lambda_c}{\lambda_k} \right)^2. \quad (\text{C13})$$

The (real) eigenvalues of \mathcal{M}_s gives 4 non-zero and 1 trivial normal mode frequencies (for $\kappa = 0$), which we shall denote as

$$\pm\omega_\pm = \pm \frac{1}{\sqrt{2}} \sqrt{(\omega_k^2 + \omega_o^2) \pm \sqrt{(\omega_k^2 - \omega_o^2)^2 + 16\lambda_k^2\omega_k\omega_o}} \quad (\text{C14})$$

one obtains the critical coupling constant

$$\lambda_c = \sqrt{\frac{\omega_k\omega_o}{4} \left(1 + \frac{\kappa^2}{\omega_k^2} \right)} \quad (\text{C15})$$

Figure 4 gives the normal mode spectrum for a resonant system with $\omega_k = \omega_o = 1.5$ and $\kappa = 0.1$ (in reduced units).

Appendix D: Evaluation of integrals in Eqs. 5 and 4

The integral in Eq 5 for the photon coincidence can be problematic to evaluate numerically given the oscillatory nature of the sinc function in $\mathcal{F}(z)$. To accomplish this, we use define a sinc-transformation based upon $\mathcal{F}(z)$ using the identity

$$\text{sinc}(z) = \frac{\sin(z)}{z} = \frac{1}{2} \int_{-1}^1 e^{ikz} dk. \quad (\text{D1})$$

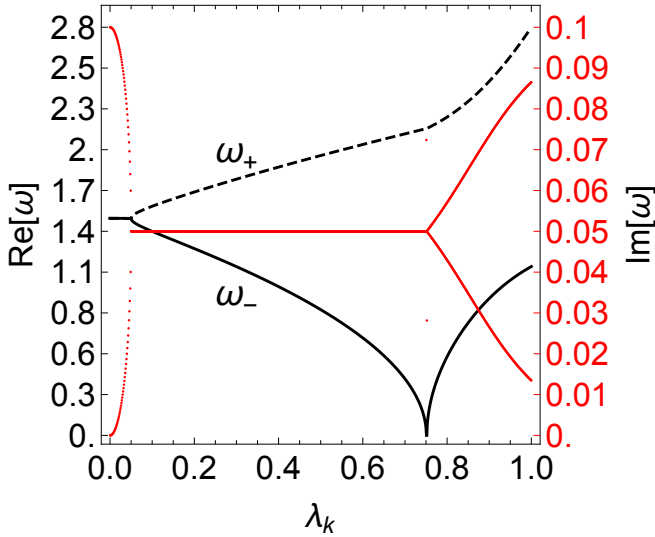


FIG. 4. **Upper and lower polariton branches.** These correspond to the eigenvalues of equation C8 for $\omega_k = \omega_o = 1.5$ and $\kappa = 0.1$ with increasing λ_k (in scaled units). The critical coupling occurs at $\lambda_k = 0.752$. A general feature of this model is that both photon and exciton-like modes decay at the same rate once $\lambda_k = \kappa/2$, corresponding to the splitting occurring at $\lambda_k = 0.05$.

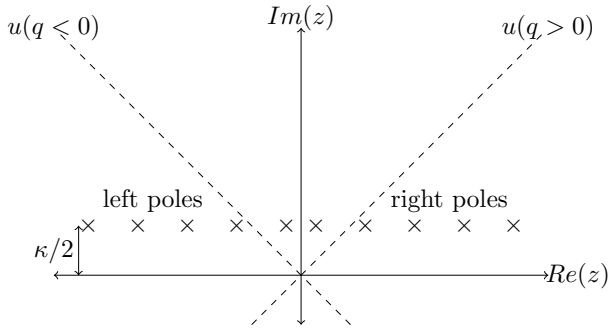


FIG. 5. **Integration axes and coordinate rotation for integrals D10-D13.**

which yields

$$\mathcal{F}(z) = \frac{1}{2} \int_{-1}^1 e^{ikbz^2} dk. \quad (\text{D2})$$

From this we can re-write each term in Eqs. 5 in the form

$$I(t) = \int_{-\infty}^{\infty} dz |\mathcal{F}(z)|^2 \mathcal{S}^*(\omega_L - z) \mathcal{S}(\omega_L + z) e^{2izt}, \quad (\text{D3})$$

$$= \frac{1}{4} \int_{-1}^1 dk \int_{-1}^1 dk' \mathcal{G}(k - k', t), \quad (\text{D4})$$

whereby we denote

$$\mathcal{G}(q, t) = \int_{-\infty}^{\infty} dz e^{-ibz^2q + 2itz} \mathcal{S}^*(\omega_L - z) \mathcal{S}(\omega_L + z). \quad (\text{D5})$$

The integrand is highly oscillatory along the z -axis; however, for non-zero $k - k' = q$, \mathcal{G} becomes a Gaussian integral under coordinate transformation obtained by completing the square:

$$-ibqz^2 + 2itz = -ibq\left(z^2 - 2\frac{t}{bq}z\right) \quad (\text{D6})$$

$$= -ibq \left[\left(z - \frac{t}{bq}\right)^2 - \left(\frac{t}{bq}\right)^2 \right] \quad (\text{D7})$$

$$= -ibq\left(z - \frac{t}{bq}\right)^2 - \frac{t^2}{ibq}. \quad (\text{D8})$$

For $q > 0$, we take $u = (\sqrt{i})(z - \frac{t}{bq})$, and for $q < 0$, we take $u = (-i\sqrt{i})(z - \frac{t}{bq})$. Solving for z yields: $z = (-i\sqrt{i})u + \frac{t}{bq}$ and $z = (\sqrt{i})u + \frac{t}{bq}$, respectively. In short, the optimal contour of the Gaussian integral is obtained by rotating by $\pi/4$ from the real-axis in the counter-clockwise direction for the case of $q > 0$ and by $\pi/4$ in the clockwise direction for the case of $q < 0$ as indicated in Fig. 5.

The spectral response $\mathcal{S}^*(\omega_L - z)\mathcal{S}(\omega_L + z)$ has a number of poles on the complex z plane above the real- z axis. We now use the residue theorem to evaluate the necessary poles which result as the contour rotates from the real axis to the complex $\pm\pi/4$ axis. The 8 second order poles, $\{\rho_n\}$, are defined by roots of the denominators $D(\omega_L - z)$ and $D(\omega_L + z)$ and located $\kappa/2$ above the real axis at locations symmetrically placed around the origin. For the counter-clockwise rotation ($q > 0$), poles included to the right of the real crossing point will be added and those to the left will be ignored ($\mathcal{P}_R(t)$); whereas for a clockwise rotation ($q < 0$), the left-hand poles will be subtracted and the right-hand poles will be ignored ($\mathcal{P}_L(t)$).

For the unique case $q = 0$, all poles are summed ($\mathcal{P}_{all}(t)$).

$$\mathcal{P}(t) = 2\pi i \sum_n \lim_{z \rightarrow \rho_n} \frac{d}{dz} \left[(z - \rho_n)^2 \mathcal{S}^*(\omega_L - z) \mathcal{S}(\omega_L + z) e^{-ibz^2q + 2izt} \right]. \quad (\text{D9})$$

Thus, we obtain

$$\mathcal{G}(q > 0, t) = e^{\frac{it^2}{bq}} \int_{-\infty}^{\infty} du e^{-bqu^2} \mathcal{S}^*(\omega_L - (-i\sqrt{i})u - \frac{t}{bq}) \mathcal{S}(\omega_L + (-i\sqrt{i})u + \frac{t}{bq}) + \mathcal{P}_R(t), \quad (\text{D10})$$

$$\mathcal{G}(q = 0, t > 0) = \mathcal{P}_{all}(t), \quad (\text{D11})$$

$$\mathcal{G}(q = 0, t < 0) = 0, \quad (\text{D12})$$

$$\mathcal{G}(q < 0, t) = e^{\frac{it^2}{bq}} \int_{-\infty}^{\infty} du e^{+bqu^2} \mathcal{S}^*(\omega_L - (\sqrt{i})u - \frac{t}{bq}) \mathcal{S}(\omega_L + (\sqrt{i})u + \frac{t}{bq}) - \mathcal{P}_L(t), \quad (\text{D13})$$

whereby \mathcal{P}_L , \mathcal{P}_R , and \mathcal{P}_{all} are summed over the left, right, or all poles, respectively. The resulting expressions are analytic (albeit lengthy) and defined by exponentials and low order polynomials. Completion of the k and k' integrals yield an exact expression for the response.

-
- ¹Eric Brannen and H. I. S. Ferguson. The Question of Correlation between Photons in Coherent Light Rays. *Nature*, 178(4531):481–482, sep 1956.
- ²R. Hanbury Brown and R. Q. Twiss. A Test of a New Type of Stellar Interferometer on Sirius. *Nature*, 178(4541):1046–1048, nov 1956.
- ³E. M. Purcell. The Question of Correlation between Photons in Coherent Light Rays. *Nature*, 178(4548):1449–1450, dec 1956.
- ⁴R. H. Brown and R. Q. Twiss. Interferometry of the Intensity Fluctuations in Light. I. Basic Theory: The Correlation between Photons in Coherent Beams of Radiation. *Proceedings of the Royal Society A: Mathematical, Physical and Engineering Sciences*, 242(1230):300–324, nov 1957.
- ⁵R. H. Brown and R. Q. Twiss. Interferometry of the Intensity Fluctuations in Light II. An Experimental Test of the Theory for Partially Coherent Light. *Proceedings of the Royal Society A: Mathematical, Physical and Engineering Sciences*, 243(1234):291–319, jan 1958.
- ⁶U. Fano. Quantum Theory of Interference Effects in the Mixing of Light from Phase-Independent Sources. *American Journal of Physics*, 29(8):539–545, aug 1961.
- ⁷H. Paul. Photon antibunching. *Reviews of Modern Physics*, 54(4):1061–1102, oct 1982.
- ⁸Nicolas Gisin, Grégoire Ribordy, Wolfgang Tittel, and Hugo Zbinden. Quantum cryptography. *Rev. Mod. Phys.*, 74:145–195, Mar 2002.
- ⁹Nicolas Gisin and Rob Thew. Quantum communication. *Nat Photon*, 1(3):165–171, 03 2007.
- ¹⁰E Knill, R Laflamme, and G J Milburn. A scheme for efficient quantum computation with linear optics. *Nature*, 409(6816):46–52, jan 2001.
- ¹¹Oleksiy Roslyak, Christoph A. Marx, and Shaul Mukamel. Non-linear spectroscopy with entangled photons: Manipulating quantum pathways of matter. *Phys. Rev. A*, 79:033832, Mar 2009.
- ¹²Gabriela Barreto Lemos, Victoria Borish, Garrett D Cole, Sven Ramelow, Radek Lapkiewicz, and Anton Zeilinger. Quantum imaging with undetected photons. *Nature*, 512(7515):409–12, aug 2014.
- ¹³J. C. López Carreño and F. P. Laussy. Excitation with quantum light. I. Exciting a harmonic oscillator. *Physical Review A*, 94(6):063825, dec 2016.
- ¹⁴J. C. López Carreño, C. Sánchez Muñoz, E. del Valle, and F. P. Laussy. Excitation with quantum light. II. Exciting a two-level system. *Physical Review A*, 94(6):063826, dec 2016.
- ¹⁵Dmitry A Kalashnikov, Anna V Paterova, Sergei P Kulik, and Leonid A Krivitsky. Infrared spectroscopy with visible light. *Nature Photonics*, 10(2):98–101, jan 2016.
- ¹⁶Dmitry A. Kalashnikov, Elizaveta V. Melik-Gaykazyan, Alexey A. Kalachev, Ye Feng Yu, Arseniy I. Kuznetsov, and Leonid A. Krivitsky. Time-resolved spectroscopy with entangled photons. arXiv://1611.02415 2016.
- ¹⁷Frank Schlawin, Konstantin E. Dorfman, Benjamin P. Fingerhut, Shaul Mukamel, and S. Mukamel. Suppression of population transport and control of exciton distributions by entangled photons. *Nature Communications*, 4:1782, apr 2013.
- ¹⁸Oleg Varnavski, Brian Pinsky, and Theodore Goodson. Entangled photon excited fluorescence in organic materials: An ultrafast coincidence detector. *The Journal of Physical Chemistry Letters*, 8(2):388–393, 2017. PMID: 28029793.
- ¹⁹W. H. Zurek. Cosmological experiments in superfluid helium? *Nature*, 317(6037):505–508, 10 1985.
- ²⁰Paul D Nation and Miles P Blencowe. The trilinear Hamiltonian: a zero-dimensional model of Hawking radiation from a quantized source. *New Journal of Physics*, 12(9):095013, 2010.
- ²¹R. H. Dicke. Coherence in spontaneous radiation processes. *Phys. Rev.*, 93:99–110, Jan 1954.
- ²²Jens Klinder, Hans Keßler, Matthias Wolke, Ludwig Mathey, and Andreas Hemmerich. Dynamical phase transition in the open dicke model. *Proceedings of the National Academy of Science*, 112:3290–3295.
- ²³C. W. Gardiner and M. J. Collett. Input and output in damped quantum systems: Quantum stochastic differential equations and the master equation. *Physical Review A*, 31(6):3761–3774, jun 1985.
- ²⁴F. Dimer, B. Estienne, A. S. Parkins, and H. J. Carmichael. Proposed realization of the dicke-model quantum phase transition in an optical cavity qed system. *Phys. Rev. A*, 75:013804, Jan 2007.
- ²⁵Wassilij Kopylov, Clive Emary, and Tobias Brandes. Counting statistics of the dicke superradiance phase transition. *Physical Review A*, 87(4):043840, 2013.
- ²⁶K Rzażewski, K Wódkiewicz, and W Żakowicz. Phase transitions, two-level atoms, and the a^2 term. *Physical Review Letters*, 35(7):432, 1975.